

This article may be downloaded for personal use only. Any other use requires prior permission of the author and AIP Publishing. This article appeared in Brian Uthe, Adam Meares, Marcin Ptaszek, and Matthew Pelton , "Solvent-dependent energy and charge transfer dynamics in hydroporphyrin-BODIPY arrays", J. Chem. Phys. 153, 074302 (2020) <https://doi.org/10.1063/5.0012737> and may be found at <https://aip.scitation.org/doi/abs/10.1063/5.0012737>.

Access to this work was provided by the University of Maryland, Baltimore County (UMBC) ScholarWorks@UMBC digital repository on the Maryland Shared Open Access (MD-SOAR) platform.

Please provide feedback

Please support the ScholarWorks@UMBC repository by emailing scholarworks-group@umbc.edu and telling us what having access to this work means to you and why it's important to you. Thank you.

**Solvent-dependent Energy and Charge Transfer Dynamics in Hydroporphyrin-
BODIPY Arrays**

4/30/20

Brian Uthe,[†] Adam Meares,[‡] Marcin Ptaszek,^{‡*} Matthew Pelton^{†*}

[†]Department of Physics

[‡]Department of Chemistry and Biochemistry

UMBC (University of Maryland, Baltimore County)

1000 Hilltop Circle

Baltimore, MD 21250

*corresponding authors

mpelton@umbc.edu (M. Pelton)

mptaszek@umbc.edu (M. Ptaszek)

Abstract

Hydroporphyrin-BODIPY arrays are a promising platform for biomedical imaging or solar energy conversion, but their photophysical properties have been relatively unexplored. In this paper, we use time-resolved fluorescence, femtosecond transient absorption spectroscopy, and density-functional-theory calculations to elucidate solvent-dependent energy- and electron-transfer processes in a series of chlorin- and bacteriochlorin-BODIPY arrays. Excitation of the BODIPY moiety results in ultrafast energy transfer to the hydroporphyrin moiety, regardless of the solvent. In toluene, energy is most likely transferred *via* the through-space Förster mechanism from the S_1 state of BODIPY to the S_2 state of hydroporphyrin. In DMF, substantially faster energy transfer is observed, which implies a contribution of the through-bond Dexter mechanism. In toluene, excited hydroporphyrin components show bright fluorescence, with quantum yield and fluorescence lifetime comparable to those of the benchmark monomer, whereas, in DMF, moderate to significant reduction of both quantum yield and fluorescence lifetime are observed. We attribute this quenching to photoinduced charge transfer from hydroporphyrin to BODIPY. No direct spectral signature of the charge-separated state is observed, which suggests that either (1) the charge-separated state decays very quickly to the ground state or (2) virtual charge-separated states, close in energy to S_1 of hydroporphyrin, promote ultrafast internal conversion.

I. Introduction

Boron complexes of dipyrromethene (BODIPYs) constitute an attractive class of chromophores, with broadly tunable absorption and emission wavelengths, high

fluorescence quantum yields, relatively long excited state lifetimes, and straightforward synthesis and functionalization.¹⁻⁴ BODIPYs have been incorporated into energy-transfer arrays, where they can function as either energy donors or acceptors.¹⁻²⁵ Multichromophoric arrays containing BODIPY have potential applications as light-harvesting materials,⁵⁻¹⁴ mimics of photosynthetic reaction centers,^{3-6,10,11,15} triplet-state photosensitizers,¹⁶⁻¹⁸ photoredox catalysts,¹⁹⁻²¹ and fluorophores for intracellular or *in vivo* imaging.²²⁻²⁵

BODIPY energy-transfer arrays often use porphyrins as energy acceptors, since the strong absorption of the BODIPY subunit around 500 nm complements the absorption features of porphyrins.^{7,26} Using hydroporphyrins (HPs) in the place of porphyrins in these arrays has the potential to broaden the range of applications, because they feature prominent absorption bands in the ultraviolet (350 – 400 nm, bacteriochlorins),²⁷ violet (400 – 430 nm, chlorins),²⁸ deep red (650 – 700 nm, chlorins), or near-infrared (> 700 nm, bacteriochlorins) spectral regions. There are substantial differences in electronic, spectral, and redox properties between porphyrins and HPs,^{27,28} so one can expect distinctive photophysical properties for BODIPY-HP arrays. However, these properties have not yet been thoroughly investigated, and applications are still under development.

In this context, we recently developed a series of BODIPY-HP (chlorin and bacteriochlorin) arrays.^{25,29-31} Excitation of the BODIPY subunit in such arrays results in efficient energy transfer (EnT) to the HP subunit and, consequently, deep-red or near-infrared fluorescence.²⁹⁻³¹ These properties enabled construction of novel types of fluorophores for *in vivo* imaging.²⁵ Optimization of the fluorescence properties of these arrays requires an understanding of the energy-transfer mechanism. Two mechanisms are

possible: Förster (or through space, TS) and Dexter (or through bond, TB) EnT.^{7,32-35} The main requirement for the TS process is a spectral overlap between donor (BODIPY) emission and acceptor (HP) absorption.³⁵ For the TB process, a conjugated linker which provides substantial electronic communication between donor and acceptor is essential.^{32,34} Lindsey *et. al.* determined that EnT in BODIPY-porphyrin arrays, where BODIPY is attached through diphenylacetylene linker, occurs predominantly *via* the TB mechanism, in < 3 ps.⁷ Similarly, Burgess *et. al.* determined sub-picosecond EnT between anthracene and BODIPY, which also implies a TB mechanism.³⁶ On the other hand, it has been demonstrated that in other BODIPY³⁷ and HP^{38,39} arrays, the TS mechanism is dominant. It is thus an open question as to what mechanism operates for various HP-BODIPY arrays.

Moreover, practical application of some of the HP-BODIPY derivatives is currently limited by quenching of their fluorescence in polar solvents. This quenching depends on the linker unit, the position of the linker attachment, and the metalation state of HP. Previously, we tentatively attributed this observation to photoinduced electron transfer (ET), $\text{BDP-HP}^* \rightarrow \text{BDP}^--\text{HP}^+$, which becomes competitive with fluorescence in solvents of high dielectric constant. Although ET is detrimental to applications of HP-BODIPY arrays as probes for fluorescence imaging, it may enable applications in solar energy conversion, because the arrays would conveniently combine light-harvesting and charge-separation capabilities.^{3,4}

It is thus important to understand whether and how ET occurs in HP-BODIPY arrays. We previously hypothesized that the most likely pathway is ET from photoexcited HPs to BODIPY,²⁹⁻³¹ ($\text{BDP-HP}^* \rightarrow \text{BDP}^--\text{HP}^+$) as the former are easier to oxidize and the latter are easier to reduce.^{27,40,41} However, hole transfer (HT, i.e. $\text{BDP}^*-\text{HP} \rightarrow \text{BDP}^--\text{HP}^+$),

which would compete with EnT, cannot be excluded. Moreover, it has been shown that BODIPY can function as either an electron acceptor or electron donor in photoinduced processes,^{3,4} so the nature of the processes responsible for quenching of the excited state in the arrays remains an open question.

Here, we applied time-resolved fluorescence, transient absorption spectroscopy, and density-functional-theory calculations to investigate dynamics of the excited state in a series of chlorin-BODIPY and bacteriochlorin-BODIPY arrays. Our observations can be understood in terms of (1) ultrafast (< 10 ps) EnT from BODIPY to HP, in both polar and non-polar solvents, and (2) subsequent ET from excited HP to BODIPY in polar solvents.

II. Experimental

Chart 1 shows the series of HP-BODIPY derivatives investigated. These derivatives include a chlorin-BODIPY dyad, **C1-BDP**,²⁹ a chlorin-BODIPY triad, **ZnC2-(BDP)₂**,²⁹ and a bacteriochlorin-BODIPY dyad, **BC1-BDP**.³⁰ As benchmark monomers, we include chlorins **C1**²⁹ and **ZnC2**,²⁹ bacteriochlorin **BC1**, and BODIPY derivative **BDP**.⁴²

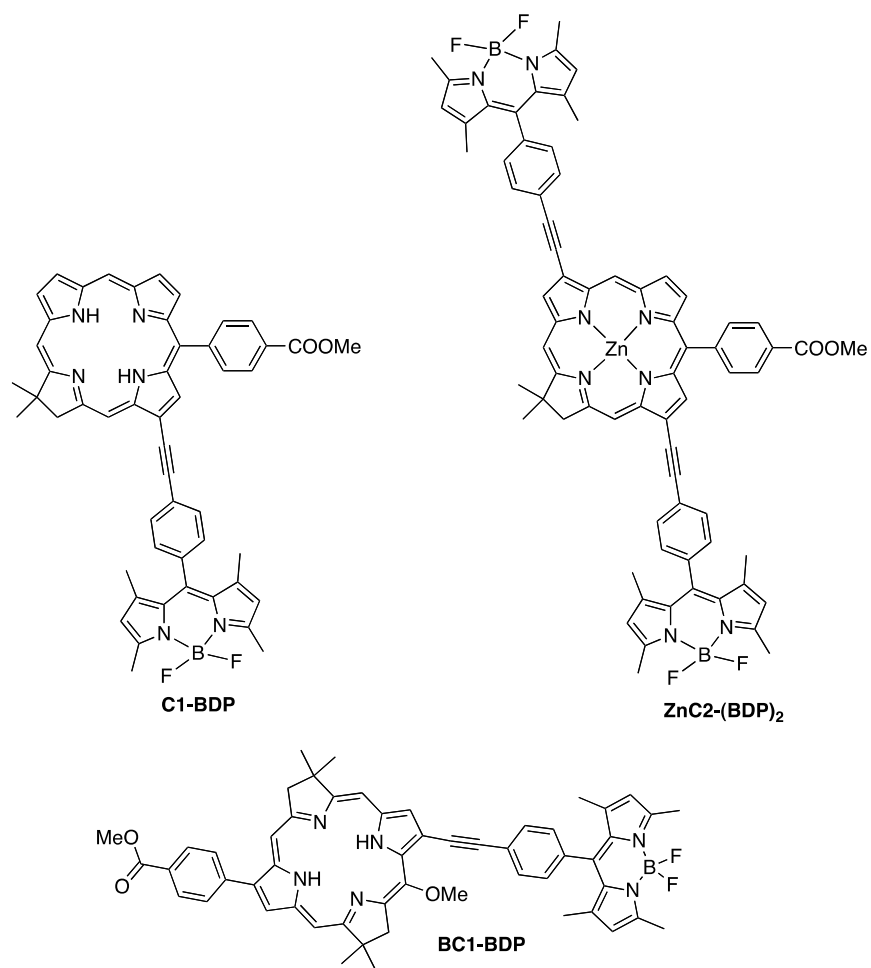


Chart 1. Structures of hydroporphyrin-BODIPY arrays.

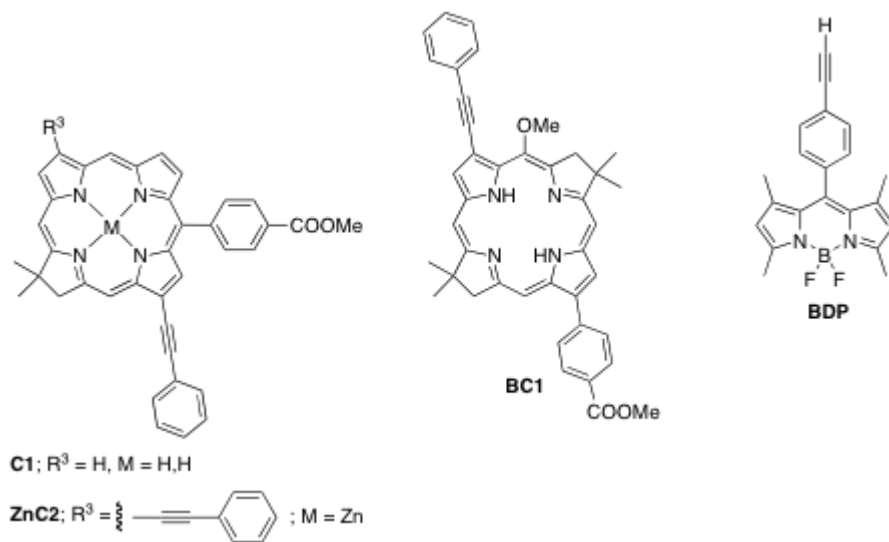
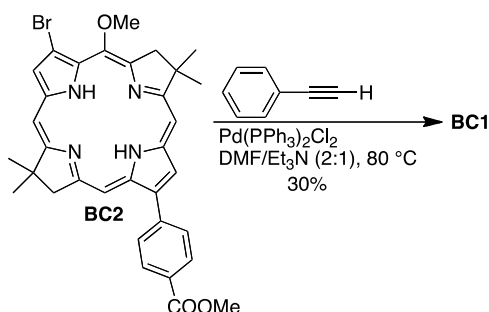


Chart 2. Structures of benchmark monomers.

Synthesis. Synthesis of arrays **C1-BDP**,²⁹ **ZnC2-(BDP)₂**,²⁹ **BC1-BDP**,³⁰ and monomers **C1**,²⁹ **ZnC2**,²⁹ and **BDP**⁴² were reported previously. 5-Methoxy-8, 8, 18, 18-tetramethyl-13-(4-methoxycarbonylphenyl)-3-phenylethynylbacteriochlorin (**BC1**) was synthesized according to Scheme 1, in the Sonogashira reaction of known **BC2**⁴³ with phenylacetylene, in 30% yield.



Scheme 1. Synthesis of hydrophorphyrin-BODIPY array **BC1**.

A solution of 3-bromo-5-methoxy-8,8,18,18-tetramethyl-13-(4-methoxycarbonylphenyl)bacteriochlorin **BC2** (15.9 mg, 25.9 μmol) in DMF (4 mL) and triethylamine (2 mL) in a Schlenk flask was subjected to two freeze-pump-thaw cycles. Then $(\text{PPh}_3)_2\text{PdCl}_2$ (3.3 mg, 4.7 μmol) was added, and a third freeze-pump-thaw cycle was performed. Next, while under flow of N_2 , phenylacetylene (9.0 μL , 82.0 μmol) was added, and the resulting mixture was stirred at 80° for 19 hours. The reaction mixture was then diluted with ethyl acetate, washed (water and brine), dried (Na_2SO_4), and concentrated. Gravity column chromatography [silica, hexanes/dichloromethane (2:1)] yielded the unidentified byproduct (first fraction, red-brown film), and the desired product (second fraction, green). ^1H NMR indicated that an impurity was present, which was removed by adding methanol (1 mL) to the product in a scintillation vial and then sonicating. Initially,

the target bacteriochlorin dissolves (solution becomes green) but it quickly saturates, at which point BC precipitates. The solvent was decanted and the process of sonication and filtration was repeated for a total of four times to fully remove the impurity. The product was isolated as a red-purple film (5.0 mg, 30%). ^1H NMR (CDCl_3 , 400 MHz): δ -1.63 (bs, 1H), -1.38 (bs, 1H), 1.93 (s, 6H), 1.96 (s, 6H), 4.06 (s, 3H), 4.34 (s, 2H), 4.44 (s, 2H), 4.51 (s, 3H), 7.41-7.45 (m, 1H), 7.47-7.51 (m, 2H), 7.85-7.89 (m, 2H), 8.24 (d, J = 8.4 Hz, 2H), 8.41 (d, J = 8.4 Hz, 2H), 8.54 (s, 1H), 8.60 (s, 1H), 8.69 (s, 1H), 8.77 (s, 1H), 8.78 (s, 1H); HRMS (ESI-FT-ICR) m/z calcd for $[\text{M}]^+$ $\text{C}_{41}\text{H}_{38}\text{N}_4\text{O}_3$ 635.3017; found 635.3014.

Calculations. DFT calculations were performed and results were visualized using Spartan 10 for Windows (Wavefunction Inc, Irvine, CA). All calculations were conducted employing the DFT B3LYP 6-31G* method. Each structure was first fully optimized in vacuum, and the MO energies were calculated, without modifying the structures, in a given solvent. For DMF-coordinated **ZnC2**, the structure included one molecule coordinated as an axial ligand to Zn(II). Förster EnT rates were calculated using PhotochemCAD software.^{44,45}

Static fluorescence. All optical measurements were made using air-equilibrated solvents at room temperature. Fluorescence quantum yield, Φ_f , was determined using tetraphenylporphyrin in toluene as a standard (Φ_f = 0.070).⁴⁶

Time-resolved fluorescence. Time-resolved fluorescence measurements were performed by time correlated single photon counting (TCSPC), using a 510-nm / 150-ps pulsed diode laser (PicoQuant PDL 800-D), an MPD PDM avalanche photodiode (MPD PDM Series), and PicoQuant PicoHarp timing electronics. Errors in the fluorescence

lifetimes were determined by fitting purely scattered laser light to estimate the instrument response function (IRF).

Transient absorption. Transient-absorption (TA) measurements were performed using a Helios spectrometer (Ultrafast Systems). Pump and probe laser pulses were derived from a regeneratively amplified Ti:Sapphire oscillator (Spectra Physics Tsunami/SpitfirePro) operating at 2 kHz. The pump pulse was produced in an optical parametric amplifier (OPA; Light Conversion TOPAS/NIRuVis). Pump laser pulse energies were between 1 μ J and 1.5 μ J. Global fitting of the TA data sets was performed by singular value decomposition, using SurfaceXplorer software (Ultrafast Systems), to obtain experimental time constants.⁴⁷

III. Results

Molecular-orbital calculations. Density-functional theory (DFT) calculations were performed to evaluate the extent of electronic interaction between the BODIPY and HP components in arrays. We focused on the HOMO and LUMO of the BODIPY component and on the HOMO-1, HOMO, LUMO, and LUMO+1 of the HP component, because these molecular orbitals (MOs) are responsible for optical transitions in the respective molecules.⁴⁸ The calculated MO energies are given in Table I.

The calculations revealed that, for each dyad, the MOs of the HP components are localized at the corresponding macrocycle, with identical symmetries as in the benchmark monomers. The relevant MO energies of the HP components are lower by $\sim 0.1 - 0.2$ eV as compared to the benchmark monomers. Similarly, the MOs of the BODIPY components

in dyads preserve the HOMO and LUMO symmetry characteristics of the monomers, with only slightly altered energies. The largely localized MOs indicate that interaction between the BODIPY and HP subunits is weak, whereas the alteration in MO energies indicates that the interaction is still non-negligible.

Table I. Molecular-orbital energies for arrays and monomers.

Compound	HOMO-1 on hydro- porphyrin component [eV]	HOMO on hydro- porphyrin component [eV]	LUMO on hydro- porphyrin component [eV]	LUMO+1 on hydro- porphyrin component [eV]	HOMO on BODIPY component [eV]	LUMO on BODIPY component [eV]
C1-BDP	-5.32	-5.12	-2.61	-2.01	-5.36	-2.36
C1	-5.21	-5.00	-2.50	-1.91	-	-
ZnC2- (BDP)₂	-5.55	-5.15	-2.79	-2.12	-5.43 -5.42	-2.42 -2.43
ZnC2	-5.35	-4.93	-2.56	-1.91	-	-
BC1- BDP	-5.21	-4.75	-2.66	-1.46	-5.34	-2.34
BC1	-5.09	-4.64	-2.54	-1.38	-	-
BDP	-	-	-	-	-5.40	-2.40

Ground state absorption and static emission properties. Absorption and emission spectra of the arrays are given in Figure 1.^{29,30} Table II summarizes the peak wavelengths

for the Q_x absorption band in BODIPY, λ_{Qx} ; the Q_y absorption band in the HPs, λ_{Qy} ; the emission wavelength, λ_{em} ; and the corresponding energy of the S_1 transition, E_{00} , calculated as the average of the maxima of the Q_y absorption and emission bands. The absorption spectrum of each array is essentially a sum of the absorption of the constituent monomers, with a slight (2-3 nm) shift of λ_{Qx} . This implies a weak inductive effect of BODIPY on HP, as predicted by DFT calculations (*vide infra*).

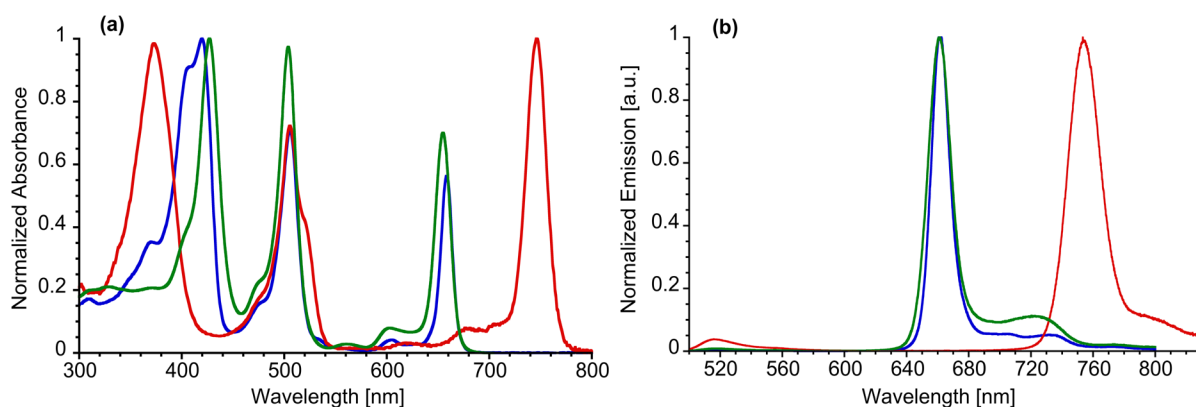


Figure 1. Normalized absorption (a) and emission (b) spectra of dyads in toluene at room temperature: **C1-BDP** (blue), **ZnC2-(BDP)₂** (green), and **BC1-BDP** (red). Emission spectra were acquired upon excitation at 490 nm.

The emission of isolated BODIPY overlaps with the absorption of the HP units, either isolated or in the arrays (see Figure S1). Excitation of each array in toluene at ~490 nm, where BODIPY absorbs nearly exclusively, results in nearly exclusive emission from the HP moiety (Figure 1b). The fluorescence quantum yields, $\Phi_f(\underline{A})$, of the HP moieties when they are directly excited at the maximum of their B band are given in Table II. The

measured values are almost identical to the quantum yields, $\Phi_f(\underline{\text{D-A}})$, of the HP components in the arrays for excitation at the maximum of BODIPY absorbance. We can estimate the efficiency of EnT more quantitatively according to $\text{ETE} = \Phi_f(\underline{\text{D-A}})/\Phi_f(\underline{\text{A}})$. The results, given in Table II, correspond to ETE of 88% or higher for all arrays, reaching as high as 97%. The estimates of high energy-transfer efficiencies are further supported by the observation that fluorescence excitation spectra, monitored at the wavelengths corresponding to HP emission, are identical with the corresponding absorption spectra. These high energy-transfer efficiencies strongly support the interpretation that quenching of BODIPY fluorescence is due to EnT to HP, rather than photoinduced ET. We note that Φ_f for arrays is slightly higher than for corresponding monomers. This provides additional evidence for some degree of electronic communication between BODIPY and HP.

When the arrays are in DMF, fluorescence remains predominantly from the HP subunit, as in toluene. Energy-transfer efficiencies are also comparable to those of the arrays in toluene. However, the fluorescence quantum yields are reduced for arrays in DMF, with the degree of reduction varying from ~ 1.4 -fold for **C1-BDP**, to ~ 3.6 -fold for **BC1-BDP** and ~ 34 -fold for **ZnC2-(BDP)₂**. This reduction is independent of excitation wavelength, and no corresponding reduction in quantum yield is observed for the corresponding HP monomer in DMF.

Table II. Absorption and emission properties of hydroporphyrin-BODIPY arrays and benchmark monomers. Numbers without parenthesis are for measurements in toluene, and numbers in parenthesis are for measurements in DMF.

Compound	λ_{Qx} [nm]	λ_{Qy} [nm]	λ_{em} [nm]	E_{00} [eV]	$\Phi_f(\underline{\text{A}})$	ETE	τ_f [ns]	k_f
----------	------------------------	------------------------	------------------------	------------------	--------------------------------	-----	---------------	-------

C1-BDP	504	657	661	1.88	0.35±0.02 (0.25±0.01)	0.97±0.07 (0.96±0.07)	8.56±0.25 (6.74±0.25)	(24.5±1.4 ns) ⁻¹ [(27.0±1.7 ns)] ⁻¹
ZnC2-(BDP)₂	504	658	661	1.88	0.37±0.02 (0.011±0.001)	0.88±0.06 (^(b))	3.59±0.25 (^(c))	(9.7±0.8 ns) ⁻¹
BC1-BDP	505	745	754	1.65	0.25±0.01 (0.07±0.004)	0.96±0.07 (0.97±0.07)	3.86±0.25 (1.25±0.25)	(15.4±1.3 ns) ⁻¹ [(17.8±3.7 ns)] ⁻¹
C1	506	656	659	1.89	0.33±0.02 (0.34±0.02)	-	9.49±0.25 (9.83±0.25)	(28.8±1.6 ns) ⁻¹ [(28.9±1.6 ns)] ⁻¹
ZnC2	519	651	656	1.90	0.33±0.02 (0.38±0.02)	-	4.17±0.25 (4.90±0.25)	(12.6±1.0 ns) ⁻¹ [(12.9±0.9 ns)] ⁻¹
BC1	520	745	750	1.66	0.22±0.01 (0.20±0.01)	-	4.30±0.25 (4.37±0.25)	(19.5±1.5 ns) ⁻¹ [(21.8±1.7 ns)] ⁻¹
BDP	504	-	515	2.44	0.71±0.04 (0.71±0.04)	-	3.03±0.25 (4.00±0.25)	(4.3±0.4 ns) ⁻¹ [(5.6±0.5 ns)] ⁻¹

^(a)ETE could not be determined accurately due to low fluorescence intensity in DMF.

^(b) Fluorescence intensity was too low for an accurate determination of the lifetime from the fitting.

Time-resolved fluorescence. Time-resolved fluorescence data are illustrated in Figure S2, and fitted fluorescence lifetimes, τ_f , are given in Table II. Also given in Table II are radiative (fluorescence) rate constants, calculated as $k_f = \Phi_f / \tau_f$.

Measured fluorescence lifetimes for the HP components of dyads in toluene are slightly shorter than the lifetimes of the corresponding monomers. Based on this slight reduction in lifetime and the slight increase in Φ_f , we calculate an increase of the radiative rate constants by ~1.2-fold (see Table II). This is, again, an indication of non-negligible electronic interaction between BODIPY and HP. Fluorescence lifetimes are reduced in

DMF, with reduction factors ranging from ~1.3-fold for **C1-BDP**, to 3-fold for **BC1-BDP**, and to > 7-fold for **ZnC2-(BDP)₂**. These factors are consistent with the corresponding reductions in fluorescence quantum yields. No reduction in fluorescence lifetime is seen for the monomers in DMF as compared to toluene, similar to the observation for quantum yields.

The results from static and time-resolved fluorescence thus both indicate that (1) there is highly efficient EnT from BODIPY to HP; and (2) when the arrays are in DMF, there is a new channel for deactivation of S₁ of HPs that competes with fluorescence (but that is not present in the corresponding monomers).

Transient absorption spectroscopy. To get further insight into the energy-transfer process from BODIPY to HP and the deactivation channel for S₁ of HPs, we have performed femtosecond transient absorption (TA) spectroscopy for each dyad. Representative transient spectra are given in Figure 2 as well as Figures S3 and S4.

Excitation of each dyad at 505 nm, corresponding to excitation of the *Q_x* absorption band in BODIPY, results in instantaneous bleaching of the *Q_x* band. This bleaching decays on time scales of 1 – 10 ps, and this decay is accompanied by a simultaneous increase of bleaching of the *Q_y* band of HP (see Figures 3 and S5). These picosecond dynamics are indicative of EnT from BODIPY to HP. The full recovery of the BODIPY bleach supports the interpretation that the quenching of BODIPY is due to EnT rather than charge transfer. This ultrafast EnT is followed by much slower decay of the *Q_y* band bleaching, corresponding to relaxation of the HP to its ground state.

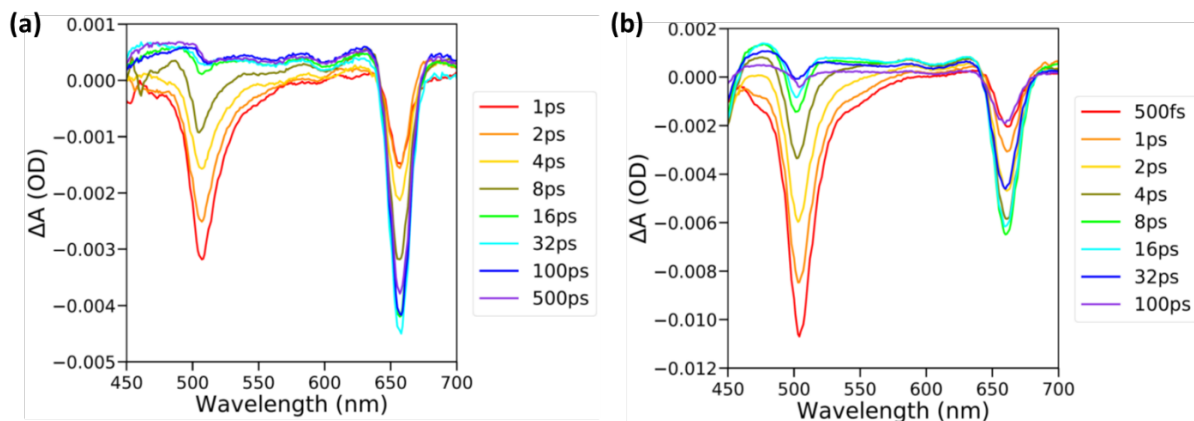


Figure 2. Representative transient-absorption spectra for different pump-probe delay times for **ZnC2-(BDP)₂** in (a) toluene and (b) DMF. Pump wavelength is 505 nm.

Time constants, τ_{Qx} , for the energy-transfer and decay processes following excitation of the Q_x absorption band in BODIPY are obtained by global fitting of the TA data. Results are summarized in Table III. Picosecond-scale energy-transfer time constants, τ_{ET} , are observed, consistent with the highly efficient EnT inferred from fluorescence data.

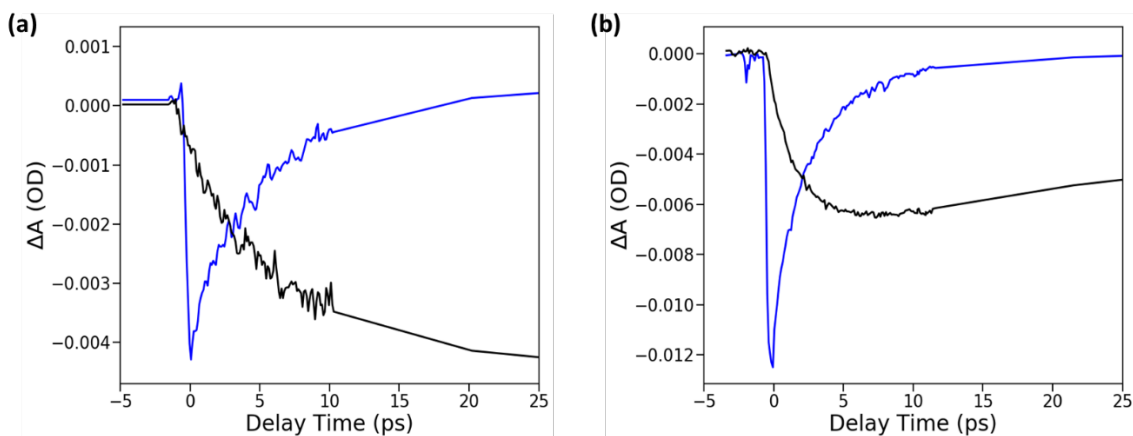


Figure 3. Representative transient-absorption kinetic traces for **ZnC2-(BDP)₂** in (a) toluene and (b) DMF. Pump wavelength is 505 nm. Blue lines are changes in absorption at

505 nm, consisting of ground-state bleaching and stimulated emission of the BODIPY component. Black lines are changes in absorption at 660 nm, consisting of ground-state bleaching and simulated emission of the chlorin component.

The relaxation time constants are generally too long to be accurately measured within the time window of the TA measurements, but are broadly consistent with the lifetimes, τ_f , measured by time-resolved fluorescence (See Table II). Significantly, both TA and time-resolved fluorescence show dramatic reduction of the S_1 lifetime of chlorin for **ZnC2-(BDP)₂** in DMF as compared to toluene, as well as a significant reduction of the S_1 lifetime for **BC1-BDP** in DMF. The TA measurements thus also indicate that these two arrays, when they are in polar solvents, have a channel for rapid depopulation of the S_1 transition of HPs.

Table III. Time constants for photoinduced processes in hydroporphyrin-BODIPY arrays, determined from transient-absorption measurements.

Compound	Solvent	$\tau_{BODIP}^{(a)}$	τ_{Qy}
C1-BDP	Toluene	8.65±.08 ps > 1.5 ns ^(b)	266±43 ps > 1.5 ns ^(a)
	DMF	5.44±0.22 ps > 1.5 ns ^(b)	401±44 ps > 1.5 ns ^(a)
ZnC2-(BDP)₂	Toluene	6.25±0.58 ps > 1.5 ns ^(b)	> 1.5 ns ^(a)
	DMF	2.39±0.34 ps	76.6±3.0 ps

		72.2 ± 3.0 ps	
BC1-BDP	Toluene	8.26 ± 0.57 ps	245 ± 33 ps
		> 1.5 ns ^(b)	> 1.5 ns ^(a)
	DMF	1.74 ± 0.08 ps 1.15 ± 0.01 ns	128 ± 13 ps 1.14 ± 0.01 ns

^(a) The longer time constant corresponds to decay of Q_x bleach that partially overlaps with BODIPY absorption.

^(b) Time constant is too large to be determined accurately.

When the pump wavelength corresponds to excitation of the Q_y absorption band in HPs, bleach only of this band is observed. This bleach, for **ZnC2-(BDP)₂** in DMF and for **BC-BDP** in DMF, decays monotonically, with a time constant, τ_{Q_y} , identical to the corresponding time constant when the Q_x absorption band is excited. (See Table III. For other cases relevant time constants could not be accurately determined). That is, the HP S_1 decay has the same time constant regardless of whether it is excited directly or through EnT from the BODIPY component. We note that the bleach recovery is biexponential, with a shorter component that has a time constant in the range of ~200 ps, and that contributes only ~15% to the overall dynamics for all compounds. (Contributions of the two decay components were estimated by taking the ratio of the preexponential factors of the corresponding terms in the biexponential fit.) This short component may be due to conformational changes in the array, such as rotation around the ethynyl moiety in the HP-BODIPY linker.⁵⁰

IV. Discussion.

Electronic communication between HP and BODIPY in arrays. Ground- and excited-state electronic communication between HP and BODIPY in arrays is expected to

have a pronounced effect on their excited-state dynamics, specifically rates and mechanisms of EnT.¹⁸ Precise determination of the degree of electronic coupling between array components would require more advanced calculations and spectroscopic measurements;¹⁸ however, our spectroscopic and computational data collectively indicate weak but non-negligible communication between HP and BODIPY in both ground and excited states. This communication is manifested by a (a) bathochromic shift of both absorption and emission maxima of HPs, (b) enhancement of radiative rate constants for HPs in arrays, and (c) alteration of MO energies in HP and BODIPY components of dyads compared to benchmark monomers. There is potentially a full π -conjugation between HP and a phenylethynyl linker, since there are no steric restrictions to prevent a coplanarity. By contrast, the BODIPY plane is nearly perpendicular to the phenyl ring of the linker, which is attached at the *meso* position; therefore, there is a negligible π -electron conjugation between HP and BODIPY. Therefore, we attribute the impact of BODIPY on the electronic properties of HP predominantly to the inductive, electron-withdrawing effect of BODIPY. However, other work^{32,34,36,39,49} indicates that there may exist other mechanisms of through-bond electronic communication in arrays, even when the conjugated linker is (nearly) perpendicular to the chromophoric π -conjugated system.

BODIPY-hydroporphyrin energy transfer. Results from fluorescence and TA measurements clearly indicate that BODIPY fluorescence is quenched by efficient EnT to hydroporphyrins. For all arrays, the rate of EnT in DMF is faster than in toluene, with the rate increasing by a factor from 4.7 (for **BC1-BDP**), to 2.6 (for **ZnC2-(BDP)₂**), to 1.6 (for **C1-BDP**). Similar increases in the rate of EnT with increasing solvent dielectric constant was previously observed for BODIPY-porphyrin arrays.⁷

The quantum efficiency of EnT can be estimated as $\phi_{\text{ET}} = 1 - \tau_{\text{BODIPY}}/\tau_f$, where τ_{BODIPY} is the time constant for decay of BODIPY band bleaching (Table III) and τ_f is the fluorescence lifetime. Efficiencies greater than 99% are estimated for all compounds. By comparing ϕ_{ET} to the EnT efficiencies (ETE) inferred from fluorescence-quantum-yield measurements (see Table II), we can infer that, if there is ET (from BODIPY to HP), it accounts for no more than 10% of BODIPY quenching. Alternatively, the difference between ETE and ϕ_{ET} could be due to an additional process through which energy is dissipated from S_1 of BODIPY in arrays, such as conformational relaxation due to rotation around the carbon-carbon triple bond in the ethyne linker.

Mechanism of energy transfer. As discussed above, absorption, emission, and computational data all indicate that there is a non-negligible electronic communication between BODIPY and HP. It would therefore be reasonable to expect that TB EnT can occur.

In order to determine whether this is the case, we calculated Förster EnT rates using the PhotochemCAD package;^{44,45} results are summarized in Table SI. Calculated rates for EnT from the S_1 state of BODIPY to the S_1 state of HP are significantly slower than experimentally measured rates. On the other hand, calculated rates for EnT from the S_1 state of BODIPY to the S_2 state of HP are as fast as or faster than experimental rates. Although the calculation of TS energy-transfer rates are affected by uncertainty in spectral parameters, particularly extinction coefficients and orientation factors,³⁸ the results provide qualitative evidence that the dominant energy-transfer mechanism in toluene is TS transfer from BODIPY to the second excited state of HP. EnT to S_2 state of the donor in arrays containing BODIPY was reported previously.⁵¹

By contrast, EnT in DMF is substantially faster than in toluene, by a factor ranging from ~ 1.6 for **C1-BDP**, to ~ 2.6 for **ZnC2-(BDP)₂**, and to ~ 4.7 for **BC1-BDP**. It is rather unlikely that changes in the absorption and emission spectra of BODIPY and HPs would result in such a significant increase in the rate of Förster EnT, as absorption and emission wavelength of arrays and benchmark monomers are very similar (See Table II). Indeed, calculated values of Förster energy transfer in DMF are nearly identical to that calculated for toluene. Therefore, we speculate that a Dexter (TB) mechanism may be a dominant pathway for energy transfer in DMF, especially for **ZnC2-(BDP)₂** and **BC1-BDP**. The more efficient TB transfer in DMF may be the result of changes in MO energies (Table SII), which can have a profound impact on the rate of TB energy transfer.^{3,34} MO energy shifts are particularly strong for **ZnC2-(BDP)₂**, due to coordination of DMF to Zn(II).

Electron transfer. The observed reduction of the S_1 lifetime and of Φ_f in a polar solvent (DMF) compared to a non-polar solvent (toluene) is consistent with a photoinduced electron or hole transfer process. In order to determine the nature of these processes, we can examine the relative HOMO and LUMO energies of HPs and BODIPY, as well as estimate the free energy ΔG for electron (ET) or hole (HT) transfers. Table I shows energies determined from DFT calculations, and Table SIII gives redox potentials from the literature, required for ΔG calculation. E^{ox} for **BC1** is not available at this point, but can be estimated as $\sim +0.30$ V, based on literature values for analogous compounds.^{40,52}

From this data, one can estimate the free energy for charge separation using the Weller equation:⁵³

$$\Delta G = e[E_{(\text{HP})}^{\text{ox}} - E_{(\text{BODIPY})}^{\text{red}}] - E_{00} + \frac{e^2}{\epsilon_s} \left(\frac{1}{2r_D} + \frac{1}{2r_A} + \frac{1}{r_{DA}} \right), \quad (1)$$

where e is the electron charge; $E^{\text{ox}}_{\text{(HP)}}$ is the half-wave oxidation potential of the corresponding HP; $E^{\text{red}}_{\text{(BODIPY)}}$ is the half-wave reduction potential of BODIPY; E^{00} is the energy of S_1 of HP (See Tables II and SIII); ϵ_s is a solvent dielectric constant; r_D and r_A are the ionic radii of donor and acceptor, respectively; and r_{DA} is the donor-acceptor center-to-center distance, respectively. The last term in the Weller equation represents the solvation of the ion-radical pair formed upon charge separation. To a first approximation, we can estimate ΔG by taking into account the half-wave redox potentials and the energy of excited states, and ignoring the relatively small contribution from solvation. Results based on this approximation are given in Table IV.

Table IV: Estimated free-energy changes, ΔG , and measured rates, k_{CS} , for photoinduced electron transfer from hydroporphyrins to BODIPY.

Reaction	$\sim\Delta G$ (eV)	k_{CS}
ZnC2*-BDP \rightarrow ZnC2⁺-BDP⁻	-0.24	$(1.3\pm0.1)\cdot10^{10}\text{ s}^{-1}$ $(78\pm3\text{ ps})^{-1}$
C1*-BDP \rightarrow C1⁺-BDP⁻	-0.09	$(3.2\pm0.6)\cdot10^7\text{ s}^{-1}$ $(31\pm7\text{ ns})^{-1}$
BC1*-BDP \rightarrow BC1⁺-BDP⁻	-0.09	$(5.4\pm1.6)\cdot10^8\text{ s}^{-1}$ $(1.8\pm0.6\text{ ns})^{-1}$

Despite all the approximations involved, our estimates of the free-energy changes for electron-transfer reactions can indicate which transfer processes are plausible. In particular, the estimates suggest that ET from photoexcited chlorin or bacteriochlorin to BODIPY is energetically feasible in polar solvents. The estimated ordering of ΔG is consistent with the extent to which fluorescence lifetimes and quantum yields are observed to be reduced in the arrays (See Table II). This conclusion is also supported by DFT

calculations, which confirm that the LUMOs of hydroporphyrins are higher in energy than the LUMO of BODIPY. We note, however, that Goutermann theory predicts that the $S_0 \rightarrow S_1$ transition for HPs is composed of 60 – 75% of the HOMO \rightarrow LUMO one-electron transition and 25 – 40% of the HOMO-1 \rightarrow LUMO+1 transition.^{27,28,48} The LUMO energy can therefore be used only as an approximate estimate of the electron-donating ability of HPs in the excited state.

Hole transfer, ($\text{BDP-HP}^* \rightarrow \text{BDP}^+ \text{-HP}^-$), is less likely to be the process responsible for quenching of the HP S_1 transition, based on the following arguments. (1) The reduction half-wave potential for BODIPY is less negative than the same potential for HPs (Table SII), which means that BODIPY is easier to reduce than chlorin or bacteriochlorin. (2) The oxidation potential for HP is less positive than for BODIPY, which means that chlorins and bacteriochlorins are easier to oxidize than BODIPY. (3) Since Zn chlorins are easier to oxidize and harder to reduce than the corresponding free base, one can expect that HT would be more pronounced for arrays containing free base chlorin (e.g. **C1-BDP**), rather than for **ZnC2-(BDP)₂**, whereas the opposite is observed experimentally. (4) The HOMO energy for BODIPY is lower than the HOMO energy for HPs, which does not support HT.

We therefore conclude that the quenching of HP fluorescence is due to ET from photoexcited HP to BODIPY. The rate of this charge-separation process, k_{CS} , can be estimated from a comparison of the excited state lifetime of the HP component in arrays in toluene, τ_{tol} , and in DMF, τ_{DMF} .

$$k_{\text{CS}} = \frac{1}{\tau_{\text{DMF}}} - \frac{1}{\tau_{\text{tol}}}. \quad (2)$$

This estimate is based on the assumption that the excited state lifetimes of HP is solvent-independent, which is supported by the observation of nearly identical lifetimes of

the corresponding monomers. For **ZnC2-(BDP)₂**, we use τ_{Qy} from Table III, rather than τ_{DMF} . Table IV gives the estimated charge-transfer rates, and Figure 4 gives an overall illustration of the most probable excited-state dynamics for BDP-HP arrays following excitation of the BODIPY moiety.

It is interesting to note that HT from photoexcited BODIPY to HP ($\text{BDP}^*\text{-HP} \rightarrow \text{BDP}^-\text{-HP}^+$) is not observed, although consideration of both redox properties and relative HOMO and LUMO energies for HP and BODIPY indicate that such a process is feasible. We speculate that such process should be significantly slower (> 70 ps, based on the rate of ET from HP to BODIPY) than energy transfer from BODIPY to HP (< 10 ps, see Table III). HT from BODIPY to HP is thus not observed because it is kinetically outcompeted by energy transfer.

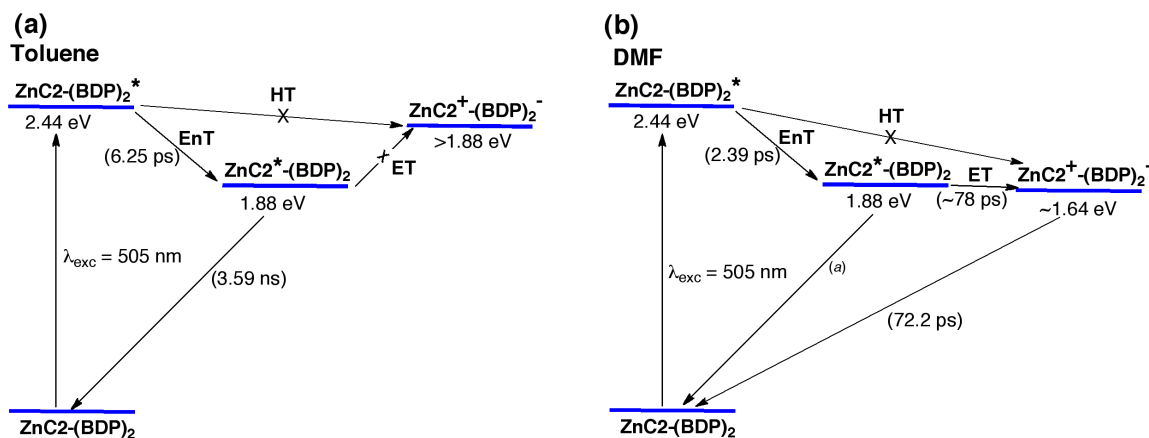


Figure 4. Schematic energy level diagram depicting photochemical processes in **ZnC2-(BDP)₂** upon excitation at 505 nm in (a) toluene and (b) DMF. EnT - energy transfer, ET – electron transfer, HT – hole transfer.

^(a)Rate constants for decay of **ZnC2*-(BDP)₂** to the ground state could not be determined, due to its very short fluorescence lifetime.

ET should result in formation of the HP radical cation $\text{HP}^{\cdot+}$ and the BODIPY radical anion $\text{BDP}^{\cdot-}$. The TA spectra (Figures 2, S2 and S3-) do not provide evidence for the formation of either radicals. The broad absorption feature between 500 nm and 700 nm observed in the TA spectra for **C1-BDP** and **BC1-BDP** is probably due to the excited state absorption of HPs, rather than a radical ion, since an identical feature is present for corresponding monomers (see Figures S6 and S7). In addition, the TA absorption features for **ZnC2-(BDP)₂** in toluene (where no quenching is observed) and in DMF (where extensive quenching is present) are almost identical (Figure 2). Moreover, the TA spectra for **ZnC2-(BDP)₂** in DMF, with $\lambda_{\text{pump}} = 650$ nm (corresponding to selective excitation of the chlorin, Figure S7) do not show noticeable ground-state bleaching of BODIPY component, even though such bleaching is expected if charge separation occurs.

These observations suggest either (1) that the cation-radical pair that results from charge separation has such a short lifetime that sufficient concentration is not generated to be observable experimentally, or (2) that the cation-radical is not an intermediate in the decay of S_1 of the HP. The latter case may be possible if a virtual charge-separated state exists whose energy is slightly higher than the HP S_1 energy. In this case, mixing of the virtual charge-separated state with the excitonic state of the HP can give rise to fast internal conversion, by intersecting the S_1 and S_0 potential energy curves.^{54,55} Similar mechanisms have been proposed to explain significant shortening of excited state lifetimes in photosynthetic special pairs⁵⁴ and in synthetic porphyrin arrays.⁵⁵

V. Conclusions

Overall, the photophysical processes occurring in hydroporphyrin-BDP arrays can be summarized using **Zn2-(BDP)₂** as an example (Figure 7). Excitation of the BDP component leads to ultrafast energy transfer to the HP component. In toluene, energy transfer most likely occurs through the Förster mechanism from S₁ of BODIPY to S₂ of HP, while in DMF the Dexter mechanism makes a substantial contribution. In non-polar solvents (toluene) a charge-separated state (HP⁻-BDP⁺) is energetically not accessible, due to the destabilization of the resulting cation-radical / anion-radical pair. In solvent of high dielectric constant (DMF), the charge-separated state becomes accessible and significantly contributes to the dynamics of excited state, by quenching S₁ of HP, either through charge separation or by enhancing intersystem crossing. No long-lived charge-separated state was detected for any of the examined arrays.

The charge-separated state results in extensive quenching of HP fluorescence in polar solvents for some arrays, which may have a detrimental impact on use of the arrays in fluorescence sensing and imaging. The results reported here clearly suggest that the effects of charge transfer are dictated by the oxidation potential of HP and the reduction potential of BODIPY. Fluorescence quenching could thus potentially be mitigated by shifting the BODIPY reduction potential to a more negative value; this, in turn, could in principle be achieved by (1) replacing the strongly electronegative fluorine substituents at boron with electron-donating substituents (as we have previously demonstrated);³⁰ or (2) installing of electron-donating substituents on the BODIPY core.⁵⁶ Similarly, installation of strongly-electron-withdrawing substituents on the 10-position of chlorin, or the 13-position of bacteriochlorin⁴⁰ would shift the HP oxidation potential to more positive values and would similarly attenuate quenching of fluorescence by charge transfer.

On the other hand, the dependence of the fluorescence quantum yield on the dielectric constant of the surroundings provides an opportunity for the development of polarity-activatable fluorophores for intracellular or *in vivo* imaging and sensing. Cells are highly heterogeneous structures, and dielectric constants vary from ~ 50 in cytoplasm to ~ 5 -10 in lipid membranes.⁵⁷ Proper tuning of the redox properties of both BODIPY and HPs will allow for precise adjustment of the degree of fluorescence quenching in environments with given dielectric constants. This, in turn, will enable the development of probes whose fluorescence is selectively activated in a target environment. Examples of such probes have been reported, and proven to be useful in intracellular fluorescence sensing and other biologically-related applications.^{56,58}

Supplementary Material. See supplementary material for additional transient absorption data and details of the energy transfer and redox calculations.

Data Availability Statement. The data that supports the findings of this study are available within the article and its supplementary material. Raw data are available from the corresponding author upon reasonable request.

Acknowledgement. M. Ptaszek thanks the National Cancer Institute of the National Institutes of Health (Award Number U01CA181628). The content of this manuscript is solely the responsibility of the authors and does not necessarily represent the official views of the National Institutes of Health.

References.

- (1) A. Loudet and K. Burgess, *Chem. Rev.* **107**, 4891-4932 (2007).
- (2) R. Ziessel and A. Harriman, *Chem. Comm.* **47**, 611-631 (2011).
- (3) M. E. El-Khouly, S. Fukuzumi, and F. D'Souza, *ChemPhysChem* **15**, 30-47 (2014).
- (4) K. Lodomenou, V. Nikolau, G. Charalambidis, A. Charisiadis, and A. G. Coutsolelos, *Comptes Rendus Chimie* **20**, 314-322 (2017).
- (5) F. D'Souza, P. M. Smith, M. E. Zandler, A. L. McCarty, M. Itou, Y. Araki, and O. Ito, *J. Am. Chem. Soc.* **126**, 7898-7907 (2004).
- (6) T. Lazarides, S. Kuhri, G. Charalambidis, M. K. Panda, D. M. Guldi, and A. G. Coutsolelos, *Inorg. Chem.* **51**, 4193-4204 (2012).
- (7) F. Li, S. I. Yang, Y. Ciringh, J. Seth, C. H. Martin III, D. L. Singh, D. Kim, R. R. Birge, D. F. Bocian, D. Holten, and J. S. Lindsey, *J. Am. Chem. Soc.* **120**, 10001-10017 (1998).
- (8) L. -B. Meng, D. Li, S. Xiong, X. -Y. Hu, L. Wang, and G. Li, *ChemComm.* **51**, 4643-4646 (2015).
- (9) G. Reddy, N. Duvva, S. Seetharaman, F. D'Souza, and L. Giribabu, *Phys. Chem. Chem. Phys.* **20**, 27418-27428 (2018).
- (10) S. Shao, M. B. Thomas, K. H. Park, Z. Mahaffey, D. Kim, and F. D'Souza, *Chem. Comm.* **54**, 54-57 (2018).
- (11) A. Bagaki, H. B. Gobeze, G. Charalambidis, A. Charisiadis, C. Stangel, V. Nikolau, A. Stergiou, N. Tagmatarchis, F. D'Souza, and A. G. Coutsolelos, *Inorg. Chem.* **56**, 10268-10280 (2017).

- (12) O. A. Bozdemir, S. Erbus-Cakmak, O. O. Ekiz, A. Dana, and E. U. Akkaya, *Angew. Chem. Int. Ed.* **50**, 10907-10912 (2011).
- (13) M. D. Yilmaz, O. A. Bozdemir, and E. U. Akkaya, *Org. Lett.* **8**, 2871-2873 (2006).
- (14) T. Bura, P. Retaileau, and R. Ziessel, *Angew. Chem. Int. Ed.* **49**, 6659-6663 (2010).
- (15) R. Canta, S. Seetharaman, E. M. Babin, P. A. Karr, and F. D'Souza, *J. Phys. Chem. A* **122**, 3780-3786 (2018).
- (16) S. S. Razi, Y. H. Koo, W. Kim, W. Yang, Z. Wang, H. Gobeze, F. D'Souza, J. Zhao, and D. Kim, *Inorg. Chem.* **57**, 4877-4890 (2018).
- (17) Z. Wang, Y. Xie, K. Xu, J. Zhao, and K. D. Glusac, *J. Phys. Chem. A* **119**, 6791-6806 (2015).
- (18) L. Huang, X. Cui, B. Therrien, and J. Zhao, *Chem. Eur. J.* **19**, 17472-17482 (2013).
- (19) B. Zheng, R. P. Sabatini, W.-F. Fu, M.-S. Eum, W. W. Brennessel, L. Wang, D. W. McCamant, and R. Eisenberg, *Proc. Natl. Acad. Sci.* **112**, E3987-E3996 (2015).
- (20) K. C. Dissanayake, P. O. Ebukuyo, Y. J. Dhahir, K. Wheeler, and H. He, *ChemComm.* **55**, 4973-4676 (2019).
- (21) A. M. Lifschitz, R. M. Young, J. Mendez-Arroyo, C. L. Stern, C. M. McGuirk, M. R. Wasielewski, and C. A. Mirkin, *Nature Commun.* **6**, 1-8 (2015).
- (22) L. Wu, A. Loudet, R. Barhoumi, R. C. Burghardt, and K. Burgess, *J. Am. Chem. Soc.* **131**, 9156-9157 (2009).
- (23) Y. Ueno, J. Jose, A. Loudet, C. Pérez-Bolivar, P. Anzenbacher Jr, and K. Burgess, *J. Am. Chem. Soc.* **133**, 51-55 (2011).

- (24) G. Ulrich, C. Goze, M. Guardigli, A. Roda, and R. Ziessel, *Angew. Chem. Int. Ed.* **44**, 3694-3698 (2005).
- (25) F. Ogata, T. Nagaya, Y. Maruoka, J. Akhigbe, A. Meares, M. Lucero, A. Satraitis, D. Fujimura, R. Okada, F. Inagaki, P. Choyke, M. Ptaszek, and H. Kobayashi, *Bioconjugate Chem.* **30**, 169-183 (2019).
- (26) T. K. Khan, M. Bröring, S. Mathur, M. Ravikanth, *Coord. Chem. Rev.* **257**, 2348-2387 (2013).
- (27) H. L. Kee, C. Kirmaier, Q. Tang, J. R. Diers, C. Muthiah, M. Taniguchi, J. K. Laha, M. Ptaszek, J. S. Lindsey, D. F. Bocian, and D. Holten, *Photochem. Photobiol.* **83**, 1125–1143 (2007).
- (28) E. Yang, C. Kirmaier, M. Krayner, M. Taniguchi, H.-J. Kim, J. R. Diers, D. F. Bocian, J. S. Lindsey, and D. Holten, *J. Phys. Chem. B* **115**(37), 10801–10816 (2011).
- (29) A. Meares, N. Santhaman, A. Satraitis, Z. Yu, and M. Ptaszek, *J. Org. Chem.* **80**, 3858-3869 (2015).
- (30) A. Meares, A. Satraitis, J. Akhigbe, N. Santhanam, S. Swaminathan, M. Ehudin, M. Ptaszek, *J. Org. Chem.* **82**, 6054-6070 (2017).
- (31) A. Meares, A. Satraitis, and M. Ptaszek, *J. Org. Chem.* **82**, 13068-13075 (2017).
- (32) C.-W. Wan, A. Burghart, J. Chen, F. Bergstrom, L. B.-A. Johansson, M. E. Wolford, T. G. Kim, M. R. Topp, R. M. Hochstrasser, and K. Burgess, *Chem. Eur. J.* **9**, 4430-4441 (2003).
- (33) S. Speiser, *Chem. Rev.* **96**, 1953-1976 (1996).

- (34) D. Holten, D. F. Bocian, and J. S. Lindsey, *Acc. Chem. Res.* **35**, 57-69 (2002).
- (35) B. Valeur, *Molecular Fluorescence: Principles and Applications* (Wiley-VCH, 2002).
- (36) T. G. Kim, C. J. Castro, A. Loudet, G.-S. Jiao, R. M. Hochstrasser, K. Burgess, and M. R. Topp, *J. Phys. Chem. A* **110**, 20-27 (2006).
- (37) A. Harriman, M. A. H. Alamiry, J. P. Hagon, D. Hablot, R. Ziessel, *Angew. Chem. Int. Ed.* **52**, 6611-6615 (2013).
- (38) C. Muthiah, H. L. Kee, J. R. Diers, D. Fan, M. Ptaszek, D. F. Bocian, D. Holten, and J. S. Lindsey, *Photochem. Photobiol.* **84**, 786–801 (2008).
- (39) M. Taniguchi, D. Ra, C. Kirmaier, E. Hindin, J. K. Schwartz, J. R. Diers, R. S. Knox, D. F. Bocian, J. S. Lindsey, D. Holten, *J. Am. Chem. Soc.* **125**, 13461–13470 (2003).
- (40) C.-Y. Chen, E. Sun, M. Fan, M. Taniguchi, B. E. McDowell, E. Yang, J. R. Diers, D. F. Bocian, D. Holten, and J. S. Lindsey, *Inorg. Chem.* **51**, 9443-9464 (2012).
- (41) C. K. Chang, L. K. Hanson, P. F. Richardson, R. Young, and J. Fajer, *Proc. Natl. Acad. Sci. USA* **78**, 2652-2656 (1981).
- (42) C. A. Wijesinghe, M. E. El-Khouly, N. K. Subbaiyan, M. Supur, M. E. Zandler, K. Ohkubo, S. Fukuzumi, and F. D'Souza, *Chem. Eur. J.* **17**, 3147-3156 (2011).
- (43) Z. Yu and M. Ptaszek, *J. Org. Chem.* **78**, 10678-10691 (2013).
- (44) H. Du, R. C. A. Fuh, J. Z. Li, L. A. Corkoran, and J. S. Lindsey, *Photochem. Photobiol.* **68**, 141-142 (1998).

- (45) M. Taniguchi, H. Du, and J. S. Lindsey, *Photochem. Photobiol.* **94**, 277-289 (2018).
- (46) A. K. Mandal, M. Taniguchi, J. R. Diers, D. M. Niedzwiedzki, C. Kirmaier, J. S. Lindsey, D. F. Bocian, and D. Holten, *J. Phys. Chem. A* **120**, 9719-9731 (2016).
- (47) E. R. Malinowski, *Factor Analysis in Chemistry* (Wiley, 1991).
- (48) M. Gouterman and G. H. Wagnière, *J. Mol Spec.* **11**, 108-127 (1963).
- (49) J. Seth, V. Palaniappan, T. E. Johnson, S. Prathapan, J. S. Lindsey, D. F. Bocian. . *Am. Chem. Soc.* **116**, 10578-10592 (1994).
- (50) R. F. Kelley, S. J. Lee, T. M. Wilson, Y. Nakamura, D. M. Tiede, A. Osuka, J. T. Hupp, M. R. Wasielewski, *J. Am. Chem. Soc.* **130**, 4277-4284 (2008).
- (51) A. Harriman, L. J. Mallon, S. Goeb, G. Ulrich, and R. Ziessel, *Chem. Eur. J.* **15**, 4553-4564 (2009).
- (52) H. L. Kee, R. J. Diers, M. Ptaszek, C. Muthiah, D. Fan, D. F. Bocian, J. S. Lindsey, J. P. Culver, and D. Holten, *Photochem. Photobiol.* **85**, 909–920 (2009).
- (53) A Weller, *Z. Phys. Chem.* **133**, 93-98 (1982).
- (54) L. M. McDowell, C. Kirmaier, and D. Holten, *Biochim. Biophys. Acta* **1020**, 239-246 (1990).
- (55) S. G. Johnson, G. J. Small, D. G. Johnson, W. A. Svec, and M. R. Wasielewski, *J. Am. Chem. Soc.* **112**, 6482-6488 (1990).
- (56) Y. Gabe, Y. Urano, K. Kikuchi, H. Kojima, and T. Nagano, *J. Am. Chem. Soc.* **126**, 3357-3367 (2004).

- (57) F.-X. Theillet, A. Binolfi, T. Frembgen-Kesner, K. Hingorani, M. Sarkar, C. Kyne, C. Li, L. Gierasch, G. J. Pielak, A. H. Elcock, A. Gershenson, and P. Selenko, *Chem. Rev.* **114**, 6661-6714 (2014).
- (58) Yogo, T.; Urano, Y.; Mizushima, A.; Sunahara, H.; Inoue, T.; Hirose, K.; Lino, M.; Kikuchi, K.; Nagano, T. Selective Photo Inactivation of Protein Function through Environment-sensitive Switching of Singlet Oxygen Generation by Photosensitizer. *Proc. Natl. Acad. Sci. U.S.A.* **2008**, *105*, 28-32.